Journal of Biomolecular NMR, 9 (1997) 105–111
ESCOM

J-Bio NMR 420

Application of multiple-quantum line narrowing with simultaneous ^{1}H and ^{13}C constant-time scalar-coupling evolution in PFG-HACANH and PFG-HACA(CO)NH triple-resonance experiments

G.V.T. Swapna, Carlos B. Rios, Zhigang Shang and Gaetano T. Montelione*

Center for Advanced Biotechnology and Medicine and Department of Molecular Biology and Biochemistry, Rutgers University, 679 Hoes Lane, Piscataway, NJ 08854-5638, U.S.A.

Received 3 April 1996
Accepted 2 December 1996

Keywords: Heteronuclear relaxation; Heteronuclear multiple-quantum coherence; Bovine pancreatic trypsin inhibitor; Bovine pancreatic ribonuclease A; Influenza virus A NS-1 protein; BPTI–trypsin complex

Summary

Many triple-resonance experiments make use of one-bond heteronuclear scalar couplings to establish connectivities among backbone and/or side-chain nuclei. In medium-sized (15–30 kDa) proteins, short transverse relaxation times of C^{α} single-quantum states limit signal-to-noise (S/N) ratios. These relaxation properties can be improved using heteronuclear multiple-quantum coherences (HMQCs) instead of heteronuclear single-quantum coherences (HSQCs) in the pulse sequence design. In slowly tumbling macromolecules, these HMQCs can exhibit significantly better transverse relaxation properties than HSQCs. However, HMQC-type experiments also exhibit resonance splittings due to multiple two- and three-bond homo- and heteronuclear scalar couplings. We describe here a family of pulsed-field gradient (PFG) HMQC-type triple-resonance experiments using simultaneous ^{1}H and ^{13}C constant-time (CT) periods to eliminate the t_1 dependence of these scalar coupling effects. These simultaneous CT PFG-(HA)CANH and PFG-(HA)CA(CO)NH HMQC-type experiments exhibit sharper resonance line widths and often have better S/N ratios than the corresponding HSQC-type experiments. Results on proteins ranging in size from 6 to 30 kDa show average methine $C^{\alpha}H$ HMQC:HSQC enhancement factors of 1.10 ± 0.15, with about 40% of the cross peaks exhibiting better S/N ratios in the simultaneous CT-HMQC versions compared with the HSQC versions.

Resonance assignments form the basis for interpreting multidimensional NMR spectra of proteins in terms of solution structure and dynamics (Wüthrich, 1986). The introduction of multidimensional triple-resonance NMR experiments has dramatically improved the speed and reliability of the assignment process (Montelione and Wagner, 1989,1990; Ikura et al., 1990; Kay et al., 1990, 1991; Boucher et al., 1992a; Bax and Grzesiek, 1993; Lyons et al., 1993). These experiments can be generally classified into two broad classes: the 'out-and-back' class of triple-resonance experiments (Ikura et al., 1990; Kay et al., 1990; Clubb and Wagner, 1992; Clubb et al., 1992a,b; Olejniczak et al., 1992; Wittekind and Mueller, 1993) in which magnetization is relayed from proton to carbon and nitrogen nuclei and then back to the originating proton for detection during the acquisition period, and the 'straight-through' class of experiments (Montelione and Wagner, 1989,1990; Kay et al., 1991; Boucher et al., 1992a; Grzesiek and Bax, 1992a,b,1993; Logan et al., 1992; Montelione et al., 1992; Clowes et al., 1993; Grzesiek et al., 1993a; Lyons and Montelione, 1993) in which magnetization pathways begin on proton [or carbon (Farmer and Venters, 1995)] nuclei and are relayed through carbon and nitrogen nuclei and then to proton nuclei different from the starting site for detection. 'Straight-through'-type experiments are especially useful when the intervening spin transfer pathway involves ^{13}C-^{13}C TOCSY-type transfers (Logan et al., 1992; Montelione et al., 1992; Grzesiek et al., 1993a; Lyons and Montelione, 1993; Lyons et al., 1993), which are not efficient enough to carry out in an 'out-and-back' fashion. On the other hand, out-and-back-type pulse schemes for the correlation

*To whom correspondence should be addressed.

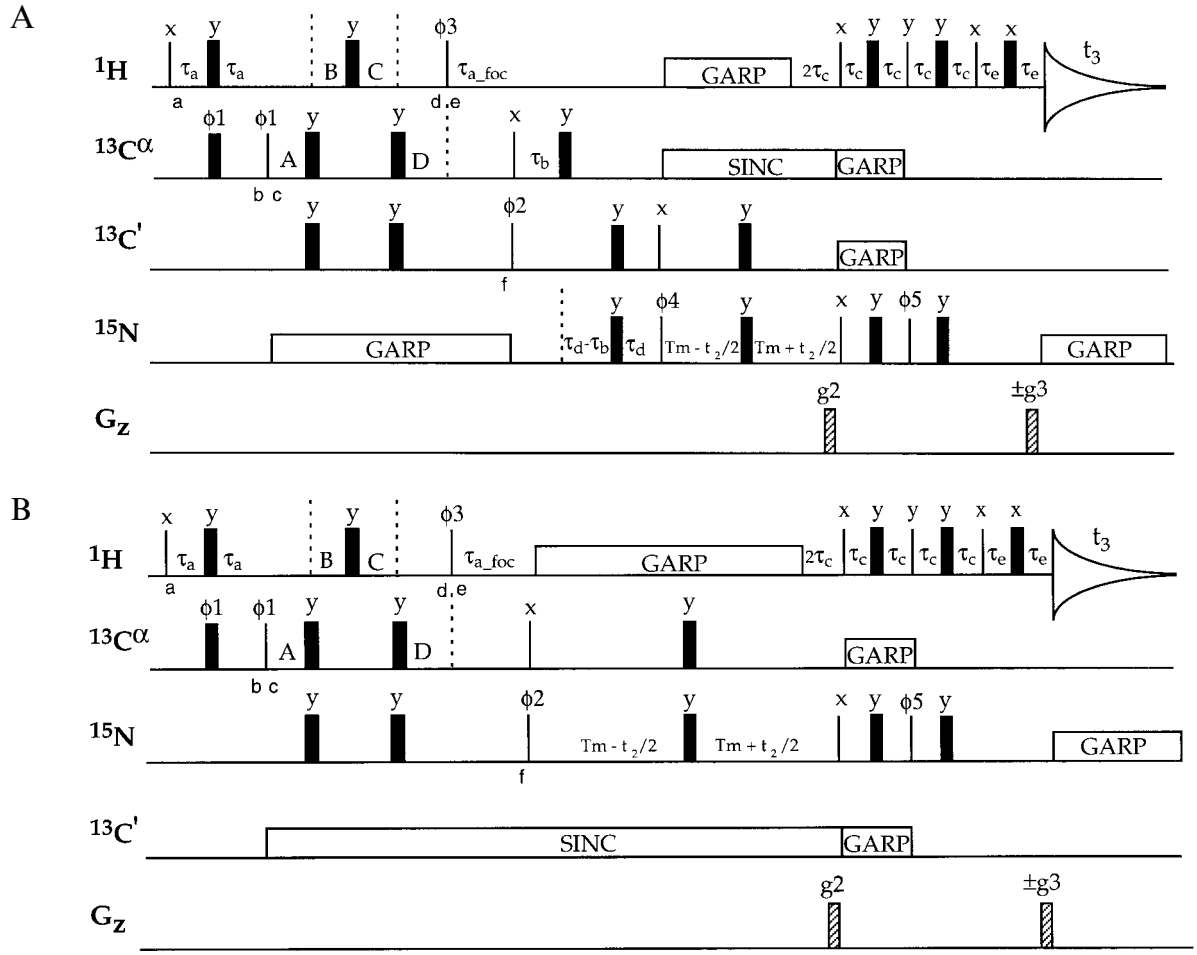

Fig. 1. Pulse sequences of 3D (A) simultaneous CT-HMQC- PFG-(HA)CA(CO)NH and (B) simultaneous CT-HMQC- PFG-(HA)CANH experiments. In both experiments the delays $A = D = (T_c + t_1/2 - \tau_{a\_foc})/2$ and $B = C = (T_c - t_1/2)/2$. The coherence transfer delays τ_{a_foc}, T_c, T_m, τ_a, τ_b, τ_c, and τ_d are adjusted as described by Feng et al. (1996), and are somewhat different depending on the protein sample; typical values are indicated in the legend of Fig. 2 for the BPTI sample and in the legend of Fig. 3 for the BPTI–trypsin complex. The pulse phases are cycled as $\phi_1 = x,-x$, $\phi_2 = x,x,-x,-x$, $\phi_3 = 4(y),4(-y)$, $\phi_4 = 8(x),8(-x)$, and the receiver phase = +,–,–,+,–,+,+,–,–,+,+,–,+,–,–,+. Pulsed-field gradients are applied along the z-axis with an amplitude of ~28 G/cm. Gradients g_2 and g_3 are used for coherence selection. Quadrature detection in the t_1 dimension was obtained in the States–TPPI manner (Marion et al., 1989), and in the t_2 dimension using gradient coherence selection with sensitivity enhancement (Kay et al., 1992). Wide-band GARP (Shaka et al., 1985) and band-selective SINC decoupling schemes were executed from waveform generators. These pulse sequences and decoupling waveforms were executed on a three-channel Varian Unity 500 NMR spectrometer equipped with a fourth synthesizer for C' decoupling, and are available by anonymous ftp from: nmrlab.cabm.rutgers.edu, or over the world-wide web at http://www-nmrlab.cabm.rutgers.edu.

of protein backbone resonances can be designed to minimize the time spent in transverse $^{13}C^{\alpha}$ magnetization states (Kay et al., 1990), which can exhibit very short relaxation times in larger proteins. For this reason, out-and-back triple-resonance experiments for the correlation of backbone resonances in proteins often exhibit better signal-to-noise ratios than the corresponding straight-through triple-resonance experiments.

One approach to overcoming this '$^{13}C^{\alpha}$ transverse relaxation problem' is to utilize ^{2}H,^{13}C,^{15}N-enriched samples in deuterium-decoupled versions of out-and-back (Grzesiek et al., 1993b; Yamazaki et al., 1994) or straight-through (Farmer and Venters, 1995) triple-resonance experiments. For ^{13}C,^{15}N-enriched proteins that are not enriched with deuterium, another possible approach to the problem is to design pulse sequences involving multiple-quantum magnetization states during the frequency evolution and coherence evolution periods. These multiple-quantum coherences can exhibit better relaxation properties (Ernst et al., 1987; Billeter et al., 1992; Grzesiek and Bax, 1995; Grzesiek et al., 1995) than the corresponding single-quantum magnetization states generally employed in triple-resonance experiments. However, one major drawback of using multiple-quantum states during indirect frequency evolution periods is that they are modulated by scalar coupling interactions with passive spins. The resulting splittings in the indirect dimension reduce the effective sensitivity and the advantages of improved relaxation rates are lost (Boucher et al., 1992b). In this communication, we describe modified versions of pulsed-field gradi-

ent (PFG) constant-time (CT) (HA)CA(CO)NH and (HA)CANH triple-resonance experiments in which the evolution of the $^{13}C^{\alpha}$ magnetization occurs via the multiple-quantum states rather than the single-quantum states. The splittings due to all homo- and heteronuclear ^2J and ^3J scalar couplings are decoupled during the t_1 evolution period using simultaneous proton and carbon CT evolution. The performance of HSQC and 'simultaneous-CT' HMQC versions of (HA)CA(CO)NH and (HA)CANH triple-resonance experiments are compared for four protein systems with molecular weights varying from 6 to 30 kDa. Some 40% of the cross peaks involving both methine and methylene C^{α} carbons exhibit enhanced signal-to-noise (S/N) ratios in the simultaneous-CT HMQC versions compared with the corresponding HSQC-type triple-resonance experiments.

For a two-spin system relaxing exclusively by intramolecular dipolar relaxation, the transverse relaxation rate (R_2) of heteronuclear single-quantum coherence (SQC) is given by (Ernst et al., 1987; Norwood, 1992):

$$R_2(SQC) = (1/4)q_{IS}[4J_{IS}(0) + J_{IS}(\omega_{oI}-\omega_{oS}) + 3J_{IS}(\omega_{oI}) + 3J_{IS}(\omega_{oS}) + 6J_{IS}(\omega_{oI}+\omega_{oS})] \quad (1)$$

while for heteronuclear multiple-quantum coherence (MQC):

$$R_2(ZQC) = (1/4)q_{IS}[3J_{IS}(\omega_{oI}) + 3J_{IS}(\omega_{oS}) + 2J_{IS}(\omega_{oI}-\omega_{oS})] \quad (2a)$$

$$R_2(DQC) = (1/4)q_{IS}[3J_{IS}(\omega_{oI}) + 3J_{IS}(\omega_{oS}) + 12J_{IS}(\omega_{oI}+\omega_{oS})] \quad (2b)$$

$$R_2(MQC) = 0.5[R_2(ZQC) + R_2(DQC)] \quad (2c)$$

where $q_{IS} = 1/10\ \gamma_I^2\ \gamma_S^2\ h^2\ r_{IS}^{-6}\ [\mu_o/4\pi]^2$, h is Planck's constant, γ_I and γ_S are nuclear gyromagnetic ratios, μ_o is the vacuum permeability constant, r_{IS} is the internuclear distance, and $J_{IS}(\omega)$'s are spectral density functions describing the molecular motion of the internuclear vector $\mathbf{r}_{IS}$. For the commonly assumed isotropic tumbling case, $J_{IS}(\omega) = 2\tau_c^{IS}/(1+(\omega_o\tau_c^{IS})^2)$, where ω_o is the Zeeman frequency of either spin I or spin S and τ_c^{IS} is the rotational correlation time of the isotropic random tumbling. In the fast motion limit (i.e. $\omega_{oS}\tau_c < \omega_{oI}\tau_c \ll 1$) of isotropic tumbling, all spectral density functions are approximately equal to one another; for heteronuclear systems, the relative relaxation rates for single-, zero-, and double-quantum coherences are 17:8:18. However, in the slow motion limit (i.e. $\omega_{oI}\tau_c > \omega_{oS}\tau_c \gg 1$, and the J(0) terms of Eqs. 2a, b and c dominate; for heteronuclear systems, the relative relaxation rates for single-, zero-, and double-quantum coherences are 4:0:0. Thus, mutual relaxation of the two spins is slowest when they are active in multiple-quantum rather than single-quantum coherences (Norwood, 1992), and significant enhancements are possible in the HMQC spectra. However, in protein C-H spin systems, the two-spin approximation used in this analysis breaks down, as dipolar interactions between protons can significantly affect ^{13}C-^1H MQ transverse relaxation rates. These interactions increase the relaxation rates of MQ coherences and reduce the relative sensitivity gain of MQC- over SQC-type experiments. Although homonuclear dipolar and other relaxation mechanisms must be accounted for in a quantitative description of MQC relaxation rates in proteins, several research groups have successfully exploited the relaxation properties of HMQCs for sensitivity enhancement in experiments designed to measure scalar coupling constants (Billeter et al., 1992; Kuboniwa et al., 1994; Grzesiek et al., 1995) and in out-and-back triple-resonance experiments for correlating protein H, N, and C backbone atoms (Boucher et al., 1992b; Seip et al., 1992).

We have applied this multiple-quantum line narrowing technique for sensitivity enhancement of PFG (HA)CA-(CO)NH and (HA)CANH triple-resonance experiments. The HSQC versions of these experiments, referred to throughout this paper, are those described previously by Feng et al. (1996), using a constant-time ^{13}C frequency labeling period. Figure 1 shows simultaneous-CT HMQC versions of these PFG-CT-(HA)CA(CO)NH and PFG-CT-(HA)CANH experiments. In short, product operator descriptions of the coherence transfer pathways for the PFG-(HA)CA(CO)NH sequence up to the end of the t_1 evolution period are:

$$H_z^{\alpha} \xrightarrow{a} -H_y^{\alpha} \xrightarrow{b} 2H_x^{\alpha}C_z^{\alpha} \xrightarrow{c} -2H_x^{\alpha}C_y^{\alpha} \xrightarrow{d} 4H_x^{\alpha}C_x^{\alpha}C_z' \xrightarrow{e} -4H_z^{\alpha}C_x^{\alpha}C_z' \xrightarrow{f} -2C_y^{\alpha}C_z' \quad (3)$$

for the simultaneous-CT HMQC (Fig. 1A) version and

$$H_z^{\alpha} \xrightarrow{a} -H_y^{\alpha} \xrightarrow{b} 2H_x^{\alpha}C_z^{\alpha} \xrightarrow{c} 2H_z^{\alpha}C_y^{\alpha} \xrightarrow{d} -2C_y^{\alpha}C_z' \quad (4)$$

for the HSQC (Fig. 1B of Feng et al., 1996) version, where H^{α}, C^{α}, C', and N are the angular momentum operators of $^1H^{\alpha}$, $^{13}C^{\alpha}$, $^{13}C'$, and ^{15}N spins, respectively. Similarly, the coherence transfer pathways for the simultaneous-CT HMQC (Fig. 1B) and HSQC (Fig. 1A of Feng et al., 1996) versions of PFG-CT-(HA)CANH up to the end of the t_1 evolution period can be described as:

$$H_z^{\alpha} \xrightarrow{a} -H_y^{\alpha} \xrightarrow{b} 2H_x^{\alpha}C_z^{\alpha} \xrightarrow{c} -2H_x^{\alpha}C_y^{\alpha} \xrightarrow{d} 4H_x^{\alpha}C_x^{\alpha}N_z \xrightarrow{e} -4H_z^{\alpha}C_x^{\alpha}N_z \xrightarrow{f} -2C_y^{\alpha}N_z \quad (5)$$

and

$$H_z^{\alpha} \xrightarrow{a} -H_y^{\alpha} \xrightarrow{b} 2H_x^{\alpha}C_z^{\alpha} \xrightarrow{c} 2H_z^{\alpha}C_y^{\alpha} \xrightarrow{d} -2C_y^{\alpha}N_z \quad (6)$$

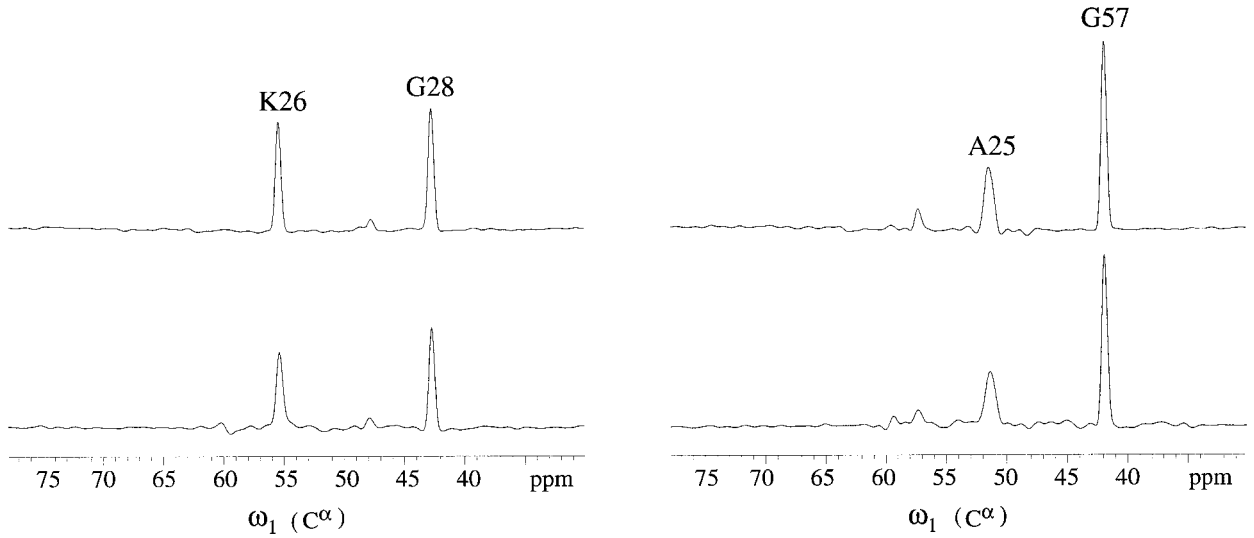

Fig. 2. Traces along ω_1 for C^{α}-H^{N}_{i+1} cross peaks in ω_1-ω_3 2D CT PFG-(HA)CA(CO)NH spectra generated using simultaneous-CT HMQC and HSQC pulse sequences. The top trace is from a simultaneous-CT HMQC PFG-(HA)CA(CO)NH spectrum (pulse sequence of Fig. 1A) and the bottom trace from our standard HSQC version (Feng et al., 1996) of the experiment. Data were obtained using a 2.0 mM sample of ^{15}N,^{13}C-enriched BPTI at pH 5.8 and 36 °C. The data sets were collected 'back-to-back', with identical total collection times (~4 h each), recycle delays, gain settings, and resolution. The data were then processed using identical Gaussian window functions. Traces are plotted with approximately identical white-noise levels. Parameters used were: $T_c = 3.5$ ms, $\tau_a = 1.6$ ms, $\tau_{a\_foc} = 1.8$ ms , $\tau_b = 3.5$ ms, $\tau_c = 2.8$ ms, $\tau_d = 14.0$ ms and $T_m = 15.0$ ms. Similar HMQC/HSQC enhancement ratios are obtained for methine sites using values $\tau_{a\_foc} = 1.8$–3.2 ms, although with these longer τ_{a_foc} values some minor phase distortions are observed for methylene Gly-X cross peaks in the HSQC (Feng et al., 1996) version of the experiment. The spectra were all acquired using 80 transients for each t_1 increment with 45 complex points in the t_1 dimension and 2048 points in the t_2 dimension. The data in the t_1 dimension were then extended by linear prediction to 128 complex points and zero-filled to 1024 complex points prior to Fourier transformation.

respectively. Accordingly, in the simultaneous-CT HMQC versions of both experiments the $^{13}C^{\alpha}$ transverse magnetization evolves as a three-spin heteronuclear multiple-quantum coherence antiphase with respect to $^{13}C'$ or ^{15}N (i.e. $4H^{\alpha}_{x,y}C^{\alpha}_{x,y}C'_z$ or $4H^{\alpha}_{x,y}C^{\alpha}_{x,y}N_z$) for a major part of the $2T_c$ period. In our experience, values of $2T_c = 6$–8 ms correspond to maxima of the coherence transfer functions for medium-sized (10–20 kDa) proteins that are of interest in this work, although smaller (<10 kDa) proteins can exhibit maxima at longer values (see the coherence-transfer curve plots in Fig. 2 of Feng et al., 1996). For proteins exhibiting optimal $2T_c$ values of 5 ms or longer, the simultaneous-CT HMQC versions of the experiments can exhibit better sensitivity than the corresponding HSQC versions.

The signal intensities in the simultaneous-CT HMQC experiment are also modulated by proton homonuclear scalar-coupling interactions during the ω_1 CT period as $\Pi_i \cos(2\pi J_{HH_i} T'_c)$, where $2T'_c = (2T_c + 2\tau_a - \tau_{a\_foc})$. For $2T'_c$ values of 6–9 ms, this effect attenuates the signal by only about 5–10%. Of course, the magnitude of attenuation due to proton homonuclear coupling depends on the values of the $J(H^{\alpha}$-$H_i)$ scalar coupling constants, the set of ϕ and χ^1 dihedral angles in the protein structure, and the value of the delay for coherence transfers, $2T'_c$. For instance, for a non-glycine H^{α} with scalar-coupling interactions $^3J(H^{\alpha}$-$H^{N})$ ~7 Hz, $^3J(H^{\alpha}$-$H^{\beta 2})$ ~4 Hz and $^3J(H^{\alpha}$-$H^{\beta 3})$ ~12 Hz, and coherence evolution periods $2T_c = 7$ ms, $\tau_a = 1.6$ ms, and $\tau_{a\_foc} = 2.5$ ms, $\Pi_i \cos(2\pi J_{HH_i} T_c) = 0.94$; i.e., the attenuation of HMQC due to the CT homonuclear scalar coupling is ~6%. The effects of heteronuclear ^1H-^{13}C couplings are refocused over the simultaneous-CT period and do not result in signal attenuation. In addition, the longitudinal relaxation properties of $^{13}C'$ and ^{15}N can modulate the efficiency of these coherence transfer pathways, although in practice the effects are small considering that the longitudinal relaxation times of typical $^{13}C'$ and ^{15}N nuclei in medium-sized proteins are long compared to the short $2T_c$ values used in these experiments.

Figure 2 shows representative ω_1-traces from ω_1-ω_3 2D spectra generated using the PFG-CT-(HA)CA(CO)NH pulse sequence on an aqueous sample of 100% uniformly ^{15}N,^{13}C-enriched bovine pancreatic trypsin inhibitor (BPTI). The traces shown provide cross sections for both non-glycine (Ala^{25} and Lys^{26}) and glycine (Gly^{28} and Gly^{57}) $^{13}C^{\alpha}$ resonances from the standard HSQC version (Feng et al., 1996) and from the simultaneous-CT HMQC experiment (Fig. 1A). Significant enhancements in signal intensities are evident in the traces of the simultaneous-CT HMQC experiment compared to those of the HSQC version. For example, the C^{α}_i-N_{i+1}-H^{N}_{i+1} cross peak for the Lys^{26}-Ala^{27} dipeptide sequence exhibits an enhancement factor of ~1.3 (compare the top and bottom traces of Fig. 2).

The performance of these simultaneous-CT HMQC PFG (HA)CA(CO)NH and (HA)CANH experiments

compared with our standard HSQC versions (Feng et al., 1996) has been quantitatively evaluated using three ^{15}N, ^{13}C-enriched protein samples with molecular weights ranging from 6 to 17 kDa. The results are listed in Table 1. The average enhancements in signal intensities and S/N ratios reported in Table 1 were calculated using all the resolved *non-glycine* C^{α} cross peaks in the corresponding ω_1-ω_3 2D spectra. The S/N ratios did not exactly match the ratios of the signal intensities, because different traces from the 2D spectra exhibit somewhat different noise levels; for this reason both intensity and S/N data are reported in Table 1. Although there is significant variation in enhancement factors along the protein sequences (data not shown), on average the cross peaks are more intense and the S/N ratios are higher in the simultaneous-CT HMQC data than in the HSQC data (Table 1). The average MQ:SQ enhancement for all resolved non-glycine correlations in the (HA)CANH and (HA)CA(CO)NH spectra for the three proteins in Table 1 is 1.10 ± 0.15. Approximately 40% of all cross peaks exhibit better S/N ratios in the simultaneous-CT HMQC spectra, and some peaks exhibit as much as 20% or more signal enhancement. On the other hand, the signal enhancement for ~60% of the methine C^{α} peaks is <1, indicating that the S/N ratios are better in the HSQC spectra than in the simultaneous-CT HMQC spectra. These data demonstrate that for some (but not all) C^{α} sites, improved sensitivity can be obtained using the simultaneous-CT HMQC versions of these triple-resonance experiments.

As expected from calculations that have been reported for BPTI (Grzesiek et al., 1995), some sites show significant MQ:SQ enhancements, while others exhibit lower S/N ratios in the MQ version of the experiment than in the SQ version. The transverse relaxation rates of the SQ coherences are mainly due to the dipolar relaxation between the C^{α} and its directly attached H^{α}. This interaction is eliminated in the multiple-quantum coherence. However, dipolar interactions between the directly attached H^{α} and other nearby protons also affect the transverse relaxation rates of MQ coherences. In situations where the advantage of eliminating the interaction between C^{α}-H^{α} is lost due to the introduction of proton–proton dipolar interactions, the signal intensities of HSQC spectra can be greater than those in the HMQC spectra. The enhancement observed at each C-H site therefore depends on the local proton density and other structural and dynamic factors that modulate the ^1H homonuclear dipolar relaxation. Thus, only a subset of peaks exhibit enhancements in the simultaneous-CT HMQC versions of these experiments.

Although only a subset of resonances are enhanced, this enhancement can sometimes be crucial for observing peaks in spectra with poor S/N. For example, Fig. 3 shows a comparison of 2D HSQC and simultaneous-CT HMQC PFG-(HA)CA(CO)NH spectra for ^{15}N,^{13}C-enriched BPTI bound to bovine β-trypsin (MW ~30 kDa). The simultaneous-CT HMQC version of the experiment provides significant improvements in the S/N ratios for many C-H sites.

Grzesiek and Bax (1995) have recently described an alternative approach, using proton spin-locking to both decouple heteronuclear scalar coupling interactions and suppress dephasing due to homonuclear proton coupling during the t_1 period of a CT-HMQC experiment. Although applied in a different experiment, this approach can provide enhancements in signal intensities for protein C^{α} methine groups comparable to those observed here. However, such spin-locking methods are susceptible to deleterious effects due to homonuclear TOCSY transfer. While TOCSY effects can be minimized by using a weak

TABLE 1
PEAK INTENSITY AND SIGNAL-TO-NOISE RATIOS IN SIMULTANEOUS-CT HMQC AND HSQC VERSIONS OF PFG-(HA)CA-(CO)NH AND PFG-(HA)CANH

Protein	MW (kDa)	sim-CT HMQC/HSQC HACA(CO)NH					sim-CT HMQC/HSQC HACANH				
		Peak intensity ratio[a]			S/N ratio[b]		Peak intensity ratio[a]			S/N ratio[b]	
		Min.	Max.	Avg.	Avg.	n[c]	Min.	Max.	Avg.	Avg.	n[c]
BPTI[d]	6.0	0.86	1.35	1.09	1.15	48	0.72	1.38	0.99	1.07	37
RNase-A[e]	14.4	0.54	1.66	1.09	0.96	74	0.57	2.51	1.28	0.96	103
NS-1(1–73)[f]	16.6	0.37	1.70	1.17	1.36	68	0.33	1.38	0.94	1.13	66

[a] Ratios of peak intensities in simultaneous-CT HMQC and HSQC versions of (HA)CA(CO)NH or (HA)CANH. Simultaneous-CT HMQC and HSQC spectra were collected 'back-to-back', with identical total collection times, recycle delays, gain settings and resolution, processed using identical Gaussian window functions, and plotted with the same vertical scale. The minimum (min.), maximum (max.) and average (avg.) ratios of the peak intensities are presented.

[b] Ratios of peak S/N ratios in simultaneous-CT HMQC and HSQC versions of (HA)CA(CO)NH or (HA)CANH. Only the average (avg.) S/N ratios are shown.

[c] Total number of cross peaks used to calculate the average enhancements. Glycine C^{α} spin systems generally show larger enhancements and are not included in these statistics.

[d] Bovine pancreatic trypsin inhibitor.

[e] Bovine pancreatic ribonuclease A.

[f] RNA-binding and dimerization domain of the nonstructural protein 1 (NS-1) from influenza A virus (Qian et al., 1995).

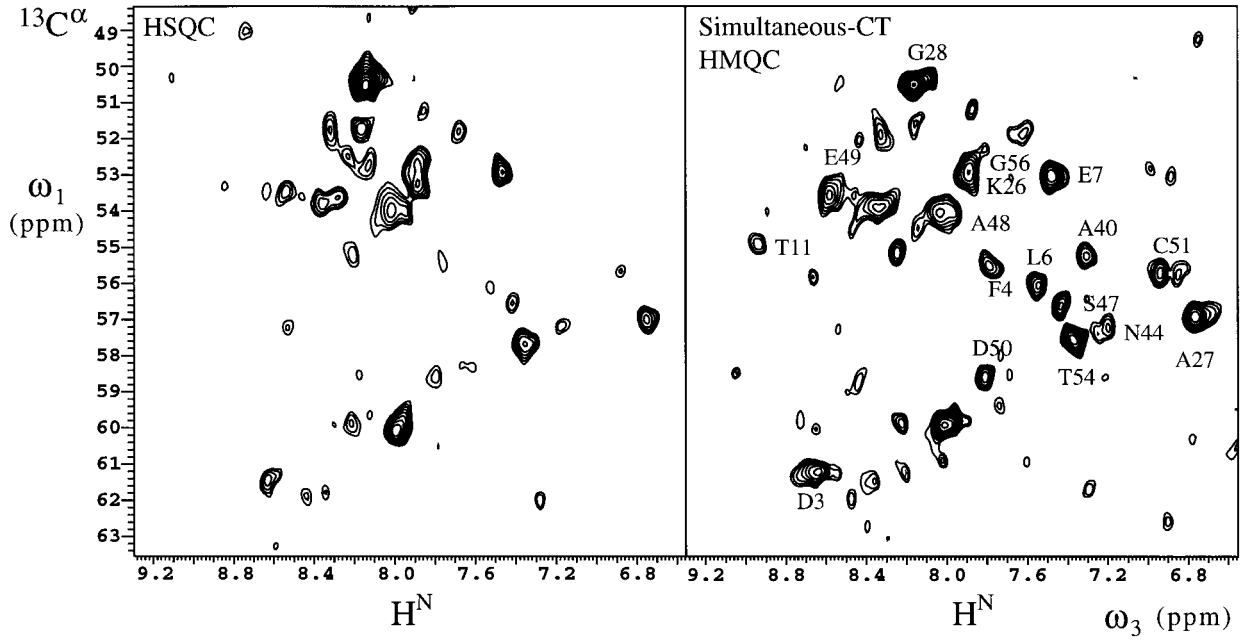

Fig. 3. 2D ω_1-ω_3 planes generated using HSQC (Feng et al., 1996) and simultaneous-CT HMQC (Fig. 1A) versions of PFG-(HA)CA(CO)NH on 1.5 mM ^{15}N,^{13}C-enriched BPTI bound to bovine β-trypsin (MW ~ 30 kDa) at pH 5.8 and 36 °C. These data sets were collected and processed under identical conditions and with identical collection times (~ 8 h) and are displayed with the same noise level. Key parameters used to acquire the data were: $T_c = 3.5$ ms, $\tau_a = 1.6$ ms, $\tau_{a\_foc} = 2.4$ ms, $\tau_b = 3.6$ ms, $\tau_c = 2.6$ ms, $\tau_d = 15.0$ ms and $T_m = 15$ ms. The spectra were acquired with 160 transients for each t_1 increment using 52 complex points in the t_1 dimension and 2048 points in the t_2 dimension. The data points along t_1 were extended by linear prediction to 128 complex points and zero-filled to 1024 complex points prior to Fourier transformation.

spin-locking field (Grzesiek and Bax, 1995), offset effects associated with the weak spin-lock field result in a second deleterious effect, namely partial refocusing of HMQCs into HSQCs due to effects of C-H scalar couplings in the tilted spin-lock frame, resulting in signal attenuation. These attenuating effects are especially severe for methylene and methyl groups. In the simultaneous-CT approach described in this communication, the ^1H-^{13}C one-, two- and three-bond scalar-coupling effects do not result in splittings in the $\omega_1 = {}^{13}C$ frequency dimension and the homonuclear ^1H-^1H and ^{13}C-^{13}C couplings have only a small attenuating effect on the signal intensity.

In conclusion, this study demonstrates the use of multiple-quantum coherences during the constant-time C^{α} evolution period of PFG-(HA)CA(CO)NH and (HA)CA-NH triple-resonance experiments. The performance of these HMQC-type triple-resonance experiments is improved by using simultaneous ^1H-^{13}C CT scalar-coupling evolution, which suppresses splittings due to homo- and heteronuclear two- and three-bond scalar couplings during the HMQC evolution period. This is especially helpful when frequency-labeling methylene and methyl carbon resonances. Our studies on three proteins in the molecular weight range 6–17 kDa show that, while average enhancements of MQ:SQ cross peaks in these triple-resonance experiments are modest (i.e. only 0–15%), and are observed for only some 40% of the sites, some sites exhibit enhancements of 20% (or more). Methylene sites of glycine residues generally exhibit larger enhancements. Thus, we view the simultaneous-CT HMQC versions of these triple-resonance experiments as useful *complements* to the previously published (Feng et al., 1996) HMQC versions. For protein systems exhibiting marginal S/N ratios in these experiments, information is gained by running *both* the HSQC and HMQC versions. Moreover, this 'simultaneous-CT HMQC' concept is quite general and should be useful in the design of many heteronuclear experiments with improved sensitivity. For example, simultaneous-CT HMQC triple-resonance pulse sequences have also been designed with frequency labeling of H^{α} (instead of C^{α}) during the t_1 period (Z. Shang, G.V.T. Swapna, C.B. Rios and G.T. Montelione, manuscript in preparation). The simultaneous-CT HMQC approach should be especially valuable for sensitivity enhancement in HCCNH- and HCC(CO)NH-COSY and TOCSY triple-resonance experiments. Efforts to develop such experiments are in progress in our laboratory.

Acknowledgements

We thank C. Biamonti, W. Feng, M. Tashiro, and R. Watson for helpful discussions and comments on the manuscript. This work was supported by grants from the National Science Foundation (MCB-9407569), a National Science Foundation Young Investigator Award (MCB-9357526 to G.T.M.), and a Camille Dreyfus Teacher-Scholar Award (to G.T.M.). We also thank the reviewers for their useful comments on the manuscript.

References

Bax, A. and Grzesiek, S. (1993) *Acc. Chem. Res.*, **26**, 131–138.

Billeter, M., Neri, D., Otting, G., Qian, Y.Q. and Wüthrich, K. (1992) *J. Biomol. NMR*, **2**, 257–274.

Boucher, W., Laue, E.D., Campbell-Burk, S. and Domaille, P.J. (1992a) *J. Am. Chem. Soc.*, **114**, 2262–2264.

Boucher, W., Laue, E.D., Campbell-Burk, S.L. and Domaille, P.J. (1992b) *J. Biomol. NMR*, **2**, 631–637.

Clowes, R.T., Boucher, W., Hardman, C.H., Domaille, P.J. and Laue, E.D. (1993) *J. Biomol. NMR*, **3**, 349–354.

Clubb, R.T. and Wagner, G. (1992) *J. Biomol. NMR*, **2**, 389–394.

Clubb, R.T., Thanabal, V. and Wagner, G. (1992a) *J. Magn. Reson.*, **97**, 213–217.

Clubb, R.T., Thanabal, V. and Wagner, G. (1992b) *J. Biomol. NMR*, **2**, 203–210.

Ernst, R.R., Bodenhausen, G. and Wokaun, A. (1987) *Principles of NMR in One and Two Dimensions*, Clarendon Press, Oxford, U.K.

Farmer II, B.T. and Venters, R.A. (1995) *J. Am. Chem. Soc.*, **117**, 4187–4188.

Feng, W., Rios, C.B. and Montelione, G.T. (1996) *J. Biomol. NMR*, **8**, 98–104.

Grzesiek, S. and Bax, A. (1992a) *J. Am. Chem. Soc.*, **114**, 6291–6293.

Grzesiek, S. and Bax, A. (1992b) *J. Magn. Reson.*, **99**, 201–207.

Grzesiek, S. and Bax, A. (1993) *J. Biomol. NMR*, **3**, 185–204.

Grzesiek, S., Anglister, J. and Bax, A. (1993a) *J. Magn. Reson.*, **B101**, 114–119.

Grzesiek, S., Anglister, J., Ren, H. and Bax, A. (1993b) *J. Am. Chem. Soc.*, **115**, 4369–4370.

Grzesiek, S. and Bax, A. (1995) *J. Biomol. NMR*, **6**, 335–339.

Grzesiek, S., Kuboniwa, H., Hinck, A.P. and Bax, A. (1995) *J. Am. Chem. Soc.*, **117**, 5312–5315.

Ikura, M., Kay, L.E. and Bax, A. (1990) *Biochemistry*, **29**, 4659–4667.

Kay, L.E., Ikura, M., Tschudin, R. and Bax, A. (1990) *J. Magn. Reson.*, **89**, 496–514.

Kay, L.E., Ikura, M. and Bax, A. (1991) *J. Magn. Reson.*, **91**, 84–92.

Kay, L.E., Keifer, P. and Saarinen, T. (1992) *J. Am. Chem. Soc.*, **114**, 10663–10665.

Kuboniwa, H., Grzesiek, S., Delaglio, F. and Bax, A. (1994) *J. Biomol. NMR*, **4**, 871–878.

Logan, T.M., Olejniczak, E.T., Xu, R.X. and Fesik, S.W. (1992) *FEBS Lett.*, **314**, 413–418.

Lyons, B.A. and Montelione, G.T. (1993) *J. Magn. Reson.*, **B101**, 206–209.

Lyons, B.A., Tashiro, M., Cedergren, L., Nilsson, B. and Montelione, G.T. (1993) *Biochemistry*, **32**, 7839–7845.

Marion, D., Ikura, M., Tschudin, R. and Bax, A. (1989) *J. Magn. Reson.*, **84**, 393–399.

Montelione, G.T. and Wagner, G. (1989) *J. Am. Chem. Soc.*, **111**, 5474–5475.

Montelione, G.T. and Wagner, G. (1990) *J. Magn. Reson.*, **87**, 183–188.

Montelione, G.T., Lyons, B.A., Emerson, S.D. and Tashiro, M. (1992) *J. Am. Chem. Soc.*, **114**, 10974–10975.

Norwood, T.J. (1992) *Prog. NMR Spectrosc.*, **24**, 295–375.

Olejniczak, E.T., Xu, R.X., Petros, A.M. and Fesik, S.W. (1992) *J. Magn. Reson.*, **100**, 444–450.

Qian, X.-Y., Chien, C.-Y., Lu, Y., Montelione, G.T. and Krug, R.M. (1995) *RNA*, **1**, 948–956.

Seip, S., Balbach, J. and Kessler, H. (1992) *J. Magn. Reson.*, **100**, 406–410.

Shaka, A.J., Barker, P.B. and Freeman, R. (1985) *J. Magn. Reson.*, **64**, 547–552.

Wittekind, M. and Mueller, L. (1993) *J. Magn. Reson.*, **B101**, 201–205.

Wüthrich, K. (1986) *NMR of Proteins and Nucleic Acids*, Wiley, New York, NY, U.S.A.

Yamazaki, T., Lee, W., Revington, M., Mattiello, D.L., Dahlquist, F.W., Arrowsmith, C.H. and Kay, L.E. (1994) *J. Am. Chem. Soc.*, **116**, 6464–6465.